

# *N*-Cavity-Magnon Polariton Blockade via Kerr Nonlinearity

Zhe-Qi Yang,<sup>1</sup> Xiao-Yu Bi,<sup>1</sup> and Zhi-Rong Zhong<sup>1,\*</sup>

<sup>1</sup>*Fujian Key Laboratory of Quantum Information and Quantum Optics,  
College of Physics and Information Engineering,  
Fuzhou University, Fuzhou, Fujian 350108, China*

(Dated: March 18, 2026)

We theoretically propose a scheme to realize a  $n$ -cavity-magnon polariton blockade in a cavity-magnon system by utilizing the Kerr nonlinearity. Cavity-magnon polaritons are hybrid quasiparticles formed by the strong coupling between cavity photons and magnons. The Kerr nonlinearity introduces anharmonicity into the polariton energy spectrum, which in turn enables the blockade effect. We demonstrate that when the external driving frequency is resonant with the transition to the  $n$ th polariton excited state, a perfect  $n$ -polariton blockade is achieved. Moreover, increasing the driving strength enhances higher-order blockade while maintaining high purity. Our work pioneers the field of cavity-magnon polariton blockade, opens a new avenue for the preparation of controllable quantum resources and holds significant potential for applications in the fields of quantum communication and quantum information processing.

Photon blockade, arising from the anharmonic energy spectrum induced by optical nonlinearity, suppresses further excitation after a single photon is generated and enables deterministic single-photon sources for quantum information technologies [1]. Conventional photon blockade (CPB) and unconventional photon blockade (UPB)—the latter originating from destructive interference between transition pathways—have been realized in diverse platforms, including cavity quantum electrodynamics (cQED) systems [2–9], cavity optomechanics [10–14], and second-order nonlinear systems [15–17]. This concept has recently been extended to multiphoton blockade, where an  $n$ -photon state is accessible while the  $(n+1)$ th excitation is suppressed, typically via Kerr nonlinearities [18–21], photon–atom coupling [22–28], or hybrid mechanisms [29–31]. Notably, two-photon blockade has already been experimentally demonstrated in driven cQED systems [32].

Magnons—the quantized quasiparticles of collective spin excitations in ferromagnetic materials such as yttrium iron garnet—have recently emerged as a promising resource for quantum technologies [33–55]. Analogous to photon blockade, magnon blockade plays a crucial role in generating nonclassical magnon states and single-magnon sources, and both conventional magnon blockade (CMB) [56–60] and unconventional magnon blockade (UMB) [61–65] have been theoretically proposed. Cavity magnon systems, based on the coupling between magnons and cavity photons, have emerged as a prominent platform and garnered sustained interest in recent years [66–71]. Particularly, several pioneering works have demonstrated that the cavity-magnon polariton (CMP), formed via the coupling between cavity photons and magnons in cavity magnon systems, exhibits highly flexible tunability and long coherence times [72–75]. CMPs typically emerge from the strong or even ultrastrong coupling between microwave cavity photons and magnons in

yttrium iron garnet (YIG) [76–80], and have been experimentally observed in a microcavity [74, 81, 82]. These features render CMPs a unique quantum resource, stimulating extensive interest and research in a broad range of fields [83–90]. However, investigations into polariton blockade have thus far been largely confined to cQED systems and remain restricted to the single-polariton or low-order regimes [91, 92]. While single-polariton blockade offers an efficient means of manipulating single quasiparticles for applications in single-particle sources and quantum information processing, its extension to the multi-polariton regime is of profound significance for exploring many-body non-classical states and constructing quantum communication networks. Given that cavity magnon systems are promising candidates for fundamental building blocks in future quantum information infrastructures, it is highly desirable to investigate  $n$ -CMP blockade ( $n$ CMPB).

In this work, we propose a scheme for realizing  $n$ CMPB via the optical Kerr effect. The interaction between the cavity mode and the magnon mode leads to the formation of hybrid polaritonic states, while the Kerr nonlinearity induces anharmonicity in the polariton energy spectrum, thereby enabling the blockade of polariton. In principle, this scheme allows for the realization of  $n$ CMPB for arbitrary  $n$ . Furthermore, in a dissipative environment, increasing the external driving strength can effectively enhance the higher-order blockade effect without compromising its purity. While single-polariton or low-order blockade schemes are limited to a small set of quantum states and thus restrict applications in quantum information and high-dimensional logic, we demonstrate a controllable blockade of arbitrary  $n$ -CMPs that enables precise manipulation of many-body nonclassical states. This mechanism provides a feasible route for high-dimensional quantum state engineering and offers a rich, controllable quantum resource for quantum information processing, quantum communication, and quantum sensing. By extending the blockade order, our work lays both experimental and theoretical foundations for high-order

\* [zhirz@fzu.edu.cn](mailto:zhirz@fzu.edu.cn)

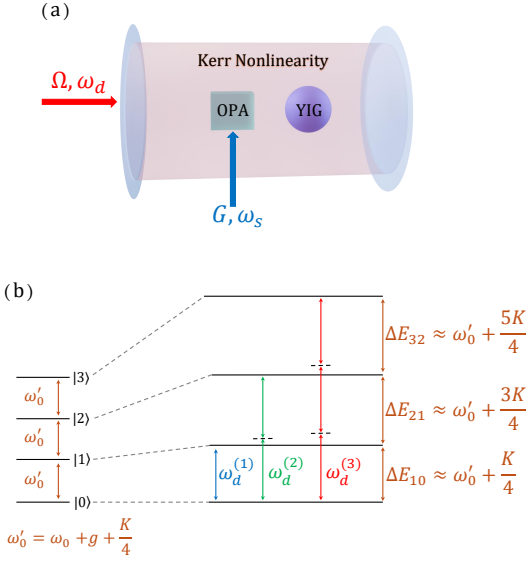


FIG. 1: (a) Sketch of the system. (b) Schematic of the  $p_+$  polariton energy levels. Here,  $\omega_d^{(n)}$  ( $n = 1, 2, 3$ ) denotes the external driving frequency required to induce the  $n$ CMPB, and it satisfies the condition given in Eq. (4).

quantum logic elements and nonlinear devices, providing a platform for constructing complex quantum networks and promising broad applications in future quantum technologies.

*Model.*—As illustrated in Fig. 1(a), we consider a Kerr nonlinear cavity consisting of a YIG sphere, an optical parametric amplifier (OPA) and a Kerr nonlinear medium. The Hamiltonian of the system can be written as ( $\hbar = 1$ )

$$H_{\text{sys}} = \omega_c a^\dagger a + \omega_m m^\dagger m + K(a^\dagger a)^2 + g(a^\dagger m + a m^\dagger) + \Omega(a^\dagger e^{-i\omega_d t} + a e^{i\omega_d t}) + G(a^{\dagger 2} e^{-i\omega_s t} + a^2 e^{i\omega_s t}), \quad (1)$$

where  $a$  ( $a^\dagger$ ) and  $m$  ( $m^\dagger$ ) represent the annihilation (creation) operators of cavity mode with frequency  $\omega_c$  and magnon mode with frequency  $\omega_m$ , respectively.  $K$  is the Kerr nonlinearity coefficient and  $g$  is the cavity-magnon coupling strength. For simplicity, we have absorbed the frequency shift of the cavity mode induced by the Kerr term into the definition of  $\omega_c$ . The cavity mode is driven by an optical laser with frequency  $\omega_d$  and amplitude  $\Omega$ , and interacts with the OPA that is externally pumped by a laser with frequency  $\omega_s$  and amplitude  $G$ . In the rotating frame with respect to  $\omega_d(a^\dagger a + m^\dagger m)$ , and utilizing  $\omega_s = 2\omega_d$ , the Hamiltonian (1) can be written as

$$H = H_0 + H_d, \\ H_0 = \Delta_c a^\dagger a + \Delta_m m^\dagger m + K(a^\dagger a)^2 + g(a^\dagger m + a m^\dagger), \\ H_d = \Omega(a^\dagger + a) + G(a^{\dagger 2} + a^2), \quad (2)$$

where  $\Delta_c = \omega_c - \omega_d$  and  $\Delta_m = \omega_m - \omega_d$ . We consider the resonant case where  $\Delta_c = \Delta_m = \Delta_0$  ( $\omega_c = \omega_m = \omega_0$ )

and define the polariton modes as  $p_+ = (a + m)/\sqrt{2}$  and  $p_- = (a - m)/\sqrt{2}$ . If we selectively drive the  $p_+$  mode by setting the driving frequency on resonance with it, the  $p_-$  mode is then far-detuned and can be safely neglected. In the strong coupling limit ( $g \gg K$ ), and under the rotating-wave approximation (RWA), Eq. (2) can be rewritten as

$$H_{\text{eff}} = \Delta_+ n_+ + \frac{K}{4} n_+^2 + \frac{\Omega}{\sqrt{2}} (p_+^\dagger + p_+) + \frac{G}{2} (p_+^{\dagger 2} + p_+^2). \quad (3)$$

where  $\Delta_+ = \Delta_0 + g + \frac{K}{4}$ ,  $n_+ = p_+^\dagger p_+$ . It can be seen from Eq. (3) that, due to the Kerr effect, namely the presence of the second term on the right-hand side, the energy spacing between adjacent polariton levels is no longer uniform. The energy-level diagram is shown in Fig. 1(b). This energy anharmonicity implies that if we set the driving detuning to be on resonance with the  $n$ th excitation ( $\omega_d = \omega_0 + g + \frac{K}{4} + \frac{nK}{4}$ ), the system will be effectively confined to the subspace with a total excitation number of  $N_+ = n$ . Any subsequent excitation to the  $N_+ = n + 1$  subspace will be strongly suppressed, as the drive is now far off-resonance from that transition frequency. Therefore, the condition for the  $n$ CMPB can be simply written as

$$\Delta_+ = -\frac{nK}{4}, n = 1, 2, 3, \dots \quad (4)$$

It is important to note that this condition can also be derived directly from the original full Hamiltonian in Eq. (1), even without performing the polariton transformation. We provide a detailed derivation in Supplemental Material [93], where we also demonstrate the validity of the effective Hamiltonian in Eq. (3).

*N-CMP blockade.*—Figures 2(a) and 2(b), as well as Figs. 2(c) and 2(d), respectively show, in the absence of dissipation, the excitation-number distributions and the time evolution of the mean excitation numbers for  $n = 2$  and  $n = 3$ . As seen in Fig. 2(a), the excitation number distribution is heavily suppressed for  $n > 2$ . Throughout the evolution,  $P_2$  peaks at a value of 0.93 while  $P_3$  remains suppressed at a maximum of just 0.04, which is a clear manifestation of the 2CMPB. In this scenario, the system's dynamics can be approximated as a Rabi oscillation between the ground state and the state  $|2\rangle$ . For the  $n = 3$  case, the blockade effect is even more pronounced: the maximum value of  $P_3$  reaches 0.95, while  $P_4$  is approximately zero, as shown in Fig. 2(c). This phenomenon is readily understood: for higher energy levels, the anharmonic energy shift between adjacent levels increases. This larger detuning from the driving frequency results in a stronger and more effective blockade.

To achieve blockade, the system must also be in the weak-driving regime, which requires the condition  $\Omega, G \ll K$  [18]. We define the fidelity of the  $n$ CMPB

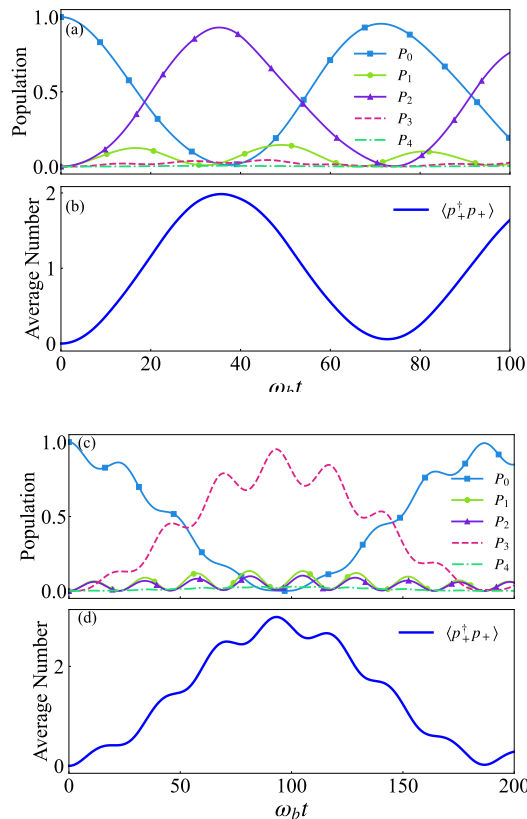


FIG. 2: Time evolution of the excitation number distribution for the (a)  $n = 2$  and (c)  $n = 3$  cases.  $P_j = \langle \psi(t) | j \rangle \langle j | \psi(t) \rangle$  ( $j = 0, 1, 2, 3, 4$ ). Here,  $|j\rangle\langle j|$  is the projection operator onto the  $j$ -th Fock state of the  $p_+$  mode. Time evolution of the mean excitation number for the (b)  $n = 2$  and (d)  $n = 3$ . The average particle number  $\langle p_+^\dagger p_+ \rangle = \langle \psi(t) | p_+^\dagger p_+ | \psi(t) \rangle$ .  $\Delta_+/g = -0.025$  in panels (a) and (b) and  $\Delta_+/g = -0.0375$  in panels (c) and (d). System parameters are  $K/g = 0.05$ , and  $\Omega/g = G/g = 0.005$ .

as

$$F_p(n) = \sum_{j=0}^n \langle \psi(t) | j \rangle \langle j | \psi(t) \rangle. \quad (5)$$

We consider the  $n$ CMPB to be successfully realized if two conditions are met: (i) the fidelity  $F_p(n) \approx 1$ , and (ii) for  $j < n$ , the fidelity  $F_p(j) \ll 1$ . If the weak-driving condition is not satisfied, the energy anharmonicity induced by the Kerr effect will be insufficient to prevent the drive from exciting the system to higher energy levels. This leads to a degradation of the fidelity  $F_p(n)$ . Therefore, in Fig. 3, we have plotted the fidelity  $F_p$  as a function of the driving strength,  $\Omega$ , for the  $n = 2$  and  $n = 3$  cases. As shown in Fig. 3(a), at the beginning of the scanned range ( $\Omega/K = 0.1$ ), the fidelity  $F_p(2)$  are both found to be approximately unity, while the fidelity  $F_p(1)$  are significantly less than 1. This confirms that the system is successfully blockaded in the total excitation subspace of  $N = 2$ . As  $\Omega/K$  increases, the aforementioned fidel-

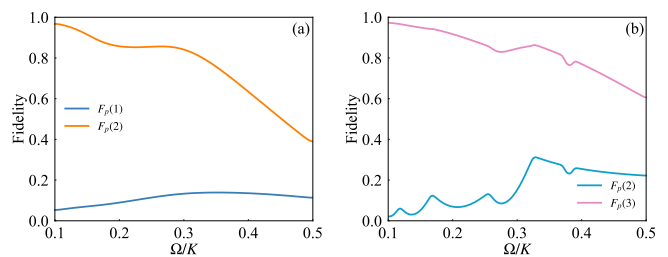


FIG. 3: Fidelity  $F_p(n)$  as a function of  $\Omega/K$  for the cases of (a)  $n = 2$  and (b)  $n = 3$ .  $\Delta_+/g = -0.025$  in panel (a) and  $\Delta_+/g = -0.0375$  in panel (b). System parameters are  $K/g = 0.05$  and  $G/g = 0.005$ .

ties exhibit a general downward trend. This indicates a failure to maintain an effective 2CMPB, as the strong drive begins to excite the system into subspaces with a total excitation number  $N > 2$ . The situation for  $n = 3$ , shown in Fig. 3(b), is qualitatively similar. However, a key difference is that the fidelity for  $n = 3$  exhibit a less pronounced decline with increasing driving strength compared to the  $n = 2$  case. This is because a stronger drive is required to overcome the energy anharmonicity and excite the system into the  $N > 3$  subspace. More significant fluctuations are observed in  $F_p(2)$  in Fig. 3(b) relative to  $F_p(1)$  in Fig. 3(a). This can be attributed to the increased population of the  $|4\rangle$  state at higher driving strengths. Transitions between the  $|2\rangle$  and  $|4\rangle$  states are subsequently induced by the two-photon drive, resulting in larger oscillations in the  $F_p(2)$  fidelity.

So far, we discussed the eigenstates and eigenvalues of  $H_0$ , established the conditions for blockade, and analyzed the corresponding evolution of the closed system under these conditions. We now extend our analysis to an open system and investigate the effects of dissipation on the dynamics. We consider the dynamics of the system to be governed by the Lindblad master equation  $\dot{\rho}(t) = -i[H_{\text{eff}}, \rho] + \kappa \mathcal{L}[p_+] \rho$ , where  $\rho$  is the system density operator,  $\kappa$  is the decay rates of the polariton modes, respectively. The Lindblad superoperator is defined as:  $\mathcal{L}[p_+] \rho = (2p_+ \rho p_+^\dagger - \rho p_+^\dagger p_+ - p_+^\dagger p_+ \rho)/2$ .

The first question to address is how the system's evolution is modified by the inclusion of dissipation. Figure 4 shows the steady-state excitation number probability distribution, as well as the dependence of the excitation number on the  $\Delta_+$ . The plotted quantities are calculated from  $\rho_{ss}$ , the steady-state solution to the master equation in the limit of  $t \rightarrow \infty$ . By analyzing Figs. 4(a) and 4(b), we can identify the conditions for various types of polariton blockade effects. For instance, the first and second dashed lines from the right in the figure correspond to the conditions for the 2CMPB and 3CMPB, respectively. The detuning values  $\Delta_+$  at these lines are in excellent agreement with the values selected for the analysis in Fig. 2. While the signatures of higher-order blockade effects are still observable in the figure, the occupation probabilities of the corresponding high-number

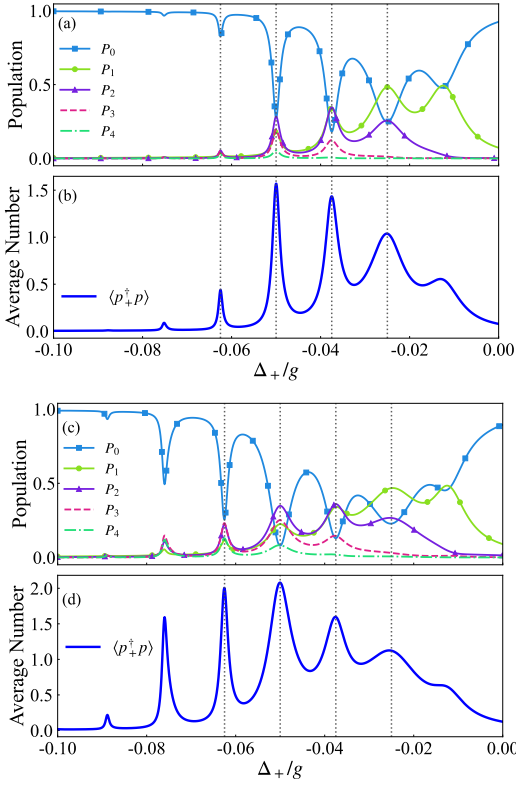


FIG. 4: Excitation number probability distribution, and mean excitation number as a function of the detuning,  $\Delta_+/g$ , in the steady state  $\rho_{ss}$ .  $P_j = \text{Tr}(|j\rangle\langle j|\rho_{ss})$  ( $j = 0, 1, 2, 3, 4$ ).  $\langle p^\dagger p \rangle = \text{Tr}(p^\dagger p \rho_{ss})$ .  $G/g = 0.005$  in panels (a) and (b) and  $G/g = 0.01$  in panels (c) and (d). The gray dashed lines in the figure (from right to left) indicate the theoretical conditions for the  $n$ PB for  $n = 2, 3, 4$ , and  $5$ , respectively. System parameters are  $K/g = 0.05$ ,  $\Omega/g = 0.01$  and  $\kappa/g = 0.001$ .

Fock states are significantly suppressed. For example, in the 4CMPB and 5CMPB cases, although the probabilities of populating the states  $|1\rangle$ ,  $|2\rangle$ ,  $|3\rangle$ , and  $|4\rangle$  are non-zero, they are dwarfed by the probability of the system remaining in the vacuum state,  $|0\rangle$ . Therefore, to achieve a high-quality, higher-order blockade, we increase the strength of the two-photon drive,  $G$ . As shown in Figs. 4(c) and 4(d), under the conditions for higher-order blockade, the mean excitation number is significantly enhanced compared to the case with the previously weaker drive. Concurrently, the population of the ground state is reduced, indicating that a more significant fraction of the system's population has been transferred to higher number states. For the 5CMPB case, for instance, the mean excitation number increases from approximately 0.5 to 2.0, and the occupation probability of the excited state becomes comparable to that of the ground state. This represents a substantial improvement in achieving a high-quality, higher-order blockade. Furthermore, a signature of a 6CMPB emerges in Figs. 4(c) and 4(d) at  $\Delta_+/g = -0.075$ . Although the ground state

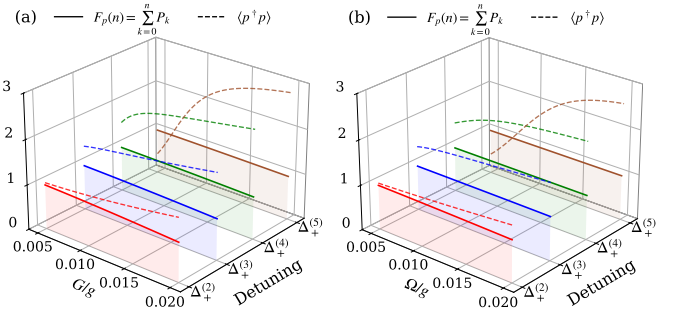


FIG. 5: Fidelities  $F_p(n)$  and the mean excitation number as a function of the drive strength (a)  $G$  and (b)  $\Omega$  for different  $n$ CMPB conditions. System parameters are  $K/g = 0.05$  and  $\kappa/g = 0.001$ .

remains the most populated state in this regime, the population of the higher excited states is still a significant enhancement over the results shown in Figs. 4(a) and 4(b). However, this approach has a potential pitfall: the strong drive may overcome the blockade and excite the system to Fock states beyond the intended target.

To investigate the influence of the drive strengths,  $\Omega$  and  $G$ , on the blockade effect in the presence of dissipation, we have plotted two key metrics in Fig. 5. Specifically, for different types of blockade, the figure shows the fidelity and the mean excitation number as a function of the corresponding drive strength. The y-axis label,  $\Delta_+$ , denotes the value of the detuning  $\Delta_+$  required to achieve the  $n$ CMPB. The values for  $n = 2, 3, 4$ , and  $5$  correspond sequentially to the four gray dashed lines shown from right to left in Fig. 4. As shown in Fig. 5(a), for the higher-order blockade effects, increasing the drive strength  $G$  leads to a significant enhancement in the mean excitation number, while the fidelity is maintained at a high level,  $F_a(n) \approx 1$ . For the 5CMPB case, for example, the mean excitation number is substantially increased from 0.44 to 2.82, while the fidelity decreases by only a negligible amount, from approximately 1.0 to 0.97. This indicates that increasing the two-photon drive strength can effectively populate higher number states without compromising the integrity of the blockade effect. It is worth noting, however, that the situation for the 2CMPB is markedly different. In this case, the mean excitation number shows no significant increase, while in contrast, the fidelity undergoes a substantial degradation, dropping from 0.99 to 0.87. A similar effect is observed for the single-photon drive,  $\Omega$ . In contrast to the two-photon drive, increasing the single-photon drive strength is less effective at enhancing the mean excitation number, as illustrated in Fig. 5(b). However, the corresponding impact on fidelity is significantly less detrimental. For instance, for the 2CMPB, the fidelity only decreases from 0.99 to 0.94, while for the 5CMPB, it is maintained at a near-unity level of 1.0. This conclusion is in apparent contradiction with our earlier discussion of Fig. 3, where we required the weak-driving condition

$\Omega, G \ll K$ . However, that requirement applies strictly to the ideal, dissipationless case, which was the focus of our analysis for Fig. 3. In a dissipative system, dissipation itself contributes to the blockade effect. This is because a larger dissipation rate makes it more difficult to populate higher-lying excited states, as they decay rapidly. Consequently, the weak-driving condition can be relaxed in the presence of dissipation. Therefore, by judiciously tuning the drive strengths  $G$  and  $\Omega$ , we can optimize the performance of a targeted polariton blockade. Additionally, by tuning the system parameters, we can selectively achieve single-photon or single-magnon blockade. A detailed discussion is provided in the Supplemental Material [93]. Our system thus exhibits high tunability and flexibility.

*Experimental feasibility and conclusions.*—Our proposal is based on a standard cavity magnon system. The frequencies of the cavity and magnon modes are chosen to be 10.1 GHz, a value typically adopted in both theoretical and experimental studies [34, 87, 94–98]. Typically, the cavity-magnon coupling strength  $g$  ranges from 1 to 100 MHz [82, 99, 100], but it can reach the GHz scale upon entering the ultrastrong coupling regime [101–103]. At present, achieving strong Kerr nonlinearity in optical cavities (e.g., with a Kerr coefficient exceeding the cavity

dissipation rate) remains highly challenging. Nevertheless, strong Kerr nonlinearities have been experimentally realized in superconducting microwave cavities [104–107], and a number of theoretical works have also adopted relatively strong Kerr nonlinearities in numerical simulations [18, 19, 29, 30, 60, 108, 109]. Therefore, the parameters employed in our numerical simulations are well within the experimentally accessible range.

In conclusion, we have proposed a scheme for realizing arbitrary  $n$ -cavity-magnon polariton blockade. By introducing Kerr nonlinearity into the system, anharmonicity is induced in the adjacent polariton energy levels, thereby enabling the polariton blockade effect. Furthermore, by analyzing the system dynamics in a dissipative environment, we find that increasing the driving strength can significantly enhance the higher-order blockade without compromising its purity. Our work transcends the limitations of previous single-polariton or low-order blockade and pioneers the field of cavity-magnon polariton blockade, providing a viable route for the precise preparation of many-body non-classical quantum states. This holds significant potential for various applications, including quantum information processing, quantum computing, and quantum sensing.

- 
- [1] P. Grangier, D. F. Walls, and K. M. Gheri, Comment on “strongly interacting photons in a nonlinear cavity”, *Phys. Rev. Lett.* **81**, 2833 (1998).
- [2] K. M. Birnbaum, A. Boca, R. Miller, A. D. Boozer, T. E. Northup, and H. J. Kimble, Photon blockade in an optical cavity with one trapped atom, *Nature (London)* **436**, 87 (2005).
- [3] Y.-x. Liu, A. Miranowicz, Y. B. Gao, J. c. v. Bajer, C. P. Sun, and F. Nori, Qubit-induced phonon blockade as a signature of quantum behavior in nanomechanical resonators, *Phys. Rev. A* **82**, 032101 (2010).
- [4] B. Dayan, A. S. Parkins, T. Aoki, E. P. Ostby, K. J. Vahala, and H. J. Kimble, A photon turnstile dynamically regulated by one atom, *Science* **319**, 1062 (2008).
- [5] Y. H. Zhou, H. Z. Shen, X. Y. Zhang, and X. X. Yi, Zero eigenvalues of a photon blockade induced by a non-hermitian hamiltonian with a gain cavity, *Phys. Rev. A* **97**, 043819 (2018).
- [6] T. Aoki, A. S. Parkins, D. J. Alton, C. A. Regal, B. Dayan, E. Ostby, K. J. Vahala, and H. J. Kimble, Efficient routing of single photons by one atom and a microtoroidal cavity, *Phys. Rev. Lett.* **102**, 083601 (2009).
- [7] J. M. Fink, A. Dombi, A. Vukics, A. Wallraff, and P. Domokos, Observation of the photon-blockade breakdown phase transition, *Phys. Rev. X* **7**, 011012 (2017).
- [8] A. J. Hoffman, S. J. Srinivasan, S. Schmidt, L. Spietz, J. Aumentado, H. E. Türeci, and A. A. Houck, Dispersive photon blockade in a superconducting circuit, *Phys. Rev. Lett.* **107**, 053602 (2011).
- [9] C. Lang, D. Bozyigit, C. Eichler, L. Steffen, J. M. Fink, A. A. Abdumalikov, M. Baur, S. Filipp, M. P. da Silva, A. Blais, and A. Wallraff, Observation of resonant photon blockade at microwave frequencies using correlation function measurements, *Phys. Rev. Lett.* **106**, 243601 (2011).
- [10] A. Nunnenkamp, K. Børkje, and S. M. Girvin, Single-photon optomechanics, *Phys. Rev. Lett.* **107**, 063602 (2011).
- [11] J.-Q. Liao and F. Nori, Photon blockade in quadratically coupled optomechanical systems, *Phys. Rev. A* **88**, 023853 (2013).
- [12] P. Rabl, Photon blockade effect in optomechanical systems, *Phys. Rev. Lett.* **107**, 063601 (2011).
- [13] H. Wang, X. Gu, Y.-x. Liu, A. Miranowicz, and F. Nori, Tunable photon blockade in a hybrid system consisting of an optomechanical device coupled to a two-level system, *Phys. Rev. A* **92**, 033806 (2015).
- [14] H. Xie, G.-W. Lin, X. Chen, Z.-H. Chen, and X.-M. Lin, Single-photon nonlinearities in a strongly driven optomechanical system with quadratic coupling, *Phys. Rev. A* **93**, 063860 (2016).
- [15] A. Majumdar and D. Gerace, Single-photon blockade in doubly resonant nanocavities with second-order nonlinearity, *Phys. Rev. B* **87**, 235319 (2013).
- [16] H. Z. Shen, Y. H. Zhou, and X. X. Yi, Quantum optical diode with semiconductor microcavities, *Phys. Rev. A* **90**, 023849 (2014).
- [17] Y. H. Zhou, X. Y. Zhang, Q. C. Wu, B. L. Ye, Z.-Q. Zhang, D. D. Zou, H. Z. Shen, and C.-P. Yang, Conventional photon blockade with a three-wave mixing, *Phys. Rev. A* **102**, 033713 (2020).
- [18] A. Miranowicz, M. Paprzycka, Y.-x. Liu, J. c. v. Bajer, and F. Nori, Two-photon and three-photon blockades in driven nonlinear systems, *Phys. Rev. A* **87**, 023809 (2013).
- [19] G.-Y. Zhang, Z.-H. Liu, J.-Q. Liao, and X.-W. Xu,

- Multiphoton blockade by frequency-matched multitone drive, *Phys. Rev. A* **112**, 053703 (2025).
- [20] R. Huang, A. Miranowicz, J.-Q. Liao, F. Nori, and H. Jing, Nonreciprocal photon blockade, *Phys. Rev. Lett.* **121**, 153601 (2018).
- [21] X. Qiao, Z. Yao, and H. Yang, Strongly enhanced photon-pair blockade with three-wave mixing by quantum interference, *Phys. Rev. A* **110**, 053702 (2024).
- [22] S. Shamailov, A. Parkins, M. Collett, and H. Carmichael, Multi-photon blockade and dressing of the dressed states, *Opt. Commun.* **283**, 766 (2010).
- [23] C. J. Zhu, Y. P. Yang, and G. S. Agarwal, Collective multiphoton blockade in cavity quantum electrodynamics, *Phys. Rev. A* **95**, 063842 (2017).
- [24] F. Zou, X.-Y. Zhang, X.-W. Xu, J.-F. Huang, and J.-Q. Liao, Multiphoton blockade in the two-photon jaynes-cummings model, *Phys. Rev. A* **102**, 053710 (2020).
- [25] C. Hamsen, K. N. Tolazzi, T. Wilk, and G. Rempe, Strong coupling between photons of two light fields mediated by one atom, *Nat. Phys.* **14**, 885 (2018).
- [26] H.-J. Li, L.-B. Fan, S. Ma, J.-Q. Liao, and C.-C. Shu, Exploring photon blockade in a two-photon jaynes-cummings model with atom and cavity drivings, *Phys. Rev. A* **110**, 043707 (2024).
- [27] Z. Haider, S. Qamar, and M. Irfan, Multiphoton blockade and antibunching in an optical cavity coupled with dipole-dipole-interacting  $\Lambda$ -type atoms, *Phys. Rev. A* **107**, 043702 (2023).
- [28] H. Lin, X. Luo, X. Wang, F. Gao, Y. Zhou, and Z. Yao, Inducing tunable conventional photon blockade and two-photon blockade in a second-order nonlinear system with two-level atoms, *Opt. Express* **32**, 23056 (2024).
- [29] J. Tang and Y. Deng, Tunable multiphoton bundles emission in a Kerr-type two-photon jaynes-cummings model, *Phys. Rev. Res.* **6**, 033247 (2024).
- [30] Y. H. Zhou, F. Minganti, W. Qin, Q.-C. Wu, J.-L. Zhao, Y.-L. Fang, F. Nori, and C.-P. Yang,  $n$ -photon blockade with an  $n$ -photon parametric drive, *Phys. Rev. A* **104**, 053718 (2021).
- [31] W. Zhang, S. Liu, S. Zhang, and H.-F. Wang, Kerr-nonlinearity enhanced photon blockades via driving a  $\delta$ -type atom, *Adv. Quantum Tech.* **6**, 2300187 (2023).
- [32] C. Hamsen, K. N. Tolazzi, T. Wilk, and G. Rempe, Two-photon blockade in an atom-driven cavity qed system, *Phys. Rev. Lett.* **118**, 133604 (2017).
- [33] M. Yu, H. Shen, and J. Li, Magnetostrictively induced stationary entanglement between two microwave fields, *Phys. Rev. Lett.* **124**, 213604 (2020).
- [34] Z. Zhang, M. O. Scully, and G. S. Agarwal, Quantum entanglement between two magnon modes via Kerr nonlinearity driven far from equilibrium, *Phys. Rev. Res.* **1**, 023021 (2019).
- [35] H. Tan and J. Li, Einstein-podolsky-rosen entanglement and asymmetric steering between distant macroscopic mechanical and magnonic systems, *Phys. Rev. Res.* **3**, 013192 (2021).
- [36] J. Li, S.-Y. Zhu, and G. S. Agarwal, Magnon-photon-phonon entanglement in cavity magnomechanics, *Phys. Rev. Lett.* **121**, 203601 (2018).
- [37] H. Yuan, Y. Cao, A. Kamra, R. A. Duine, and P. Yan, Quantum magnonics: When magnon spintronics meets quantum information science, *Phys. Rep.* **965**, 1 (2022).
- [38] J. Li, S.-Y. Zhu, and G. S. Agarwal, Squeezed states of magnons and phonons in cavity magnomechanics, *Phys. Rev. A* **99**, 021801 (2019).
- [39] Z.-Y. Fan, H. Qian, X. Zuo, and J. Li, Entangling ferromagnetic magnons with an atomic ensemble via optomagnomechanics, *Phys. Rev. A* **108**, 023501 (2023).
- [40] M. Asjad, J. Li, S.-Y. Zhu, and J. You, Magnon squeezing enhanced ground-state cooling in cavity magnomechanics, *Fundament. Res.* **3**, 3 (2023).
- [41] Z.-X. Yang, L. Wang, Y.-M. Liu, D.-Y. Wang, C.-H. Bai, S. Zhang, and H.-F. Wang, Ground state cooling of magnomechanical resonator in pt-symmetric cavity magnomechanical system at room temperature, *Front. Phys.* **15**, 52504 (2020).
- [42] Q.-K. Wan, H.-L. Shi, and X.-W. Guan, Quantum-enhanced metrology in cavity magnonics, *Phys. Rev. B* **109**, L041301 (2024).
- [43] G. Flower, M. Goryachev, J. Bourhill, and M. E. Tobar, Experimental implementations of cavity-magnon systems: from ultra strong coupling to applications in precision measurement, *New J. Phys.* **21**, 095004 (2019).
- [44] Q. Cai, J. Liao, B. Shen, G. Guo, and Q. Zhou, Microwave quantum illumination via cavity magnonics, *Phys. Rev. A* **103**, 052419 (2021).
- [45] Y. Cao and P. Yan, Exceptional magnetic sensitivity of  $\mathcal{PT}$ -symmetric cavity magnon polaritons, *Phys. Rev. B* **99**, 214415 (2019).
- [46] M. S. Ebrahimi, A. Motazedifard, and M. B. Harouni, Single-quadrature quantum magnetometry in cavity electromagnonics, *Phys. Rev. A* **103**, 062605 (2021).
- [47] X. Zhang, C.-L. Zou, N. Zhu, F. Marquardt, L. Jiang, and H. X. Tang, Magnon dark modes and gradient memory, *Nat. Commun.* **6**, 8914 (2015).
- [48] R.-C. Shen, Y.-P. Wang, J. Li, S.-Y. Zhu, G. S. Agarwal, and J. Q. You, Long-time memory and ternary logic gate using a multistable cavity magnonic system, *Phys. Rev. Lett.* **127**, 183202 (2021).
- [49] A. Osada, R. Hisatomi, A. Noguchi, Y. Tabuchi, R. Yamazaki, K. Usami, M. Sadgrove, R. Yalla, M. Nomura, and Y. Nakamura, Cavity optomagnonics with spin-orbit coupled photons, *Phys. Rev. Lett.* **116**, 223601 (2016).
- [50] J. A. Haigh, A. Nunnenkamp, A. J. Ramsay, and A. J. Ferguson, Triple-resonant brillouin light scattering in magneto-optical cavities, *Phys. Rev. Lett.* **117**, 133602 (2016).
- [51] R. Hisatomi, A. Osada, Y. Tabuchi, T. Ishikawa, A. Noguchi, R. Yamazaki, K. Usami, and Y. Nakamura, Bidirectional conversion between microwave and light via ferromagnetic magnons, *Phys. Rev. B* **93**, 174427 (2016).
- [52] Y. Xiao and K. Xia, Dissipation-induced magnon-photon entanglement in a squeezed vacuum reservoir, *Phys. Rev. B* **111**, 064414 (2025).
- [53] G. Liu, G. Li, H. Tan, and J. Li, Magnon cat states in a cavity-magnon-qubit system via two-magnon driving and dissipation, *Phys. Rev. A* **112**, 023709 (2025).
- [54] H. R. Baghshahi, M. J. Faghihi, and M. Moslehi, Generation of bipartite entanglement in a dissipative cavity magnomechanical system, *Sci. Rep.* **15**, 26981 (2025).
- [55] J. Shuai, B. Kim, J. Kim, R. Bhavsar, and S.-K. Kim, Reconfigurable control of coherence, dissipation, and nonreciprocity in cavity magnonics, *Sci. Rep.* **15**, 30893 (2025).

- [56] Z.-X. Liu, H. Xiong, and Y. Wu, Magnon blockade in a hybrid ferromagnet-superconductor quantum system, *Phys. Rev. B* **100**, 134421 (2019).
- [57] J.-k. Xie, S.-l. Ma, and F.-l. Li, Quantum-interference-enhanced magnon blockade in an yttrium-iron-garnet sphere coupled to superconducting circuits, *Phys. Rev. A* **101**, 042331 (2020).
- [58] C. Zhao, X. Li, S. Chao, R. Peng, C. Li, and L. Zhou, Simultaneous blockade of a photon, phonon, and magnon induced by a two-level atom, *Phys. Rev. A* **101**, 063838 (2020).
- [59] Y. jun Xu, T. le Yang, L. Lin, and J. Song, Conventional and unconventional magnon blockades in a qubit-magnon hybrid quantum system, *J. Opt. Soc. Am. B* **38**, 876 (2021).
- [60] Z. Ding, Y.-P. Gao, and Y. Zhang, Magnon blockade in a strongly coupled nonlinear cavity-magnon system, *J. Opt. Soc. Am. B* **41**, 332 (2024).
- [61] X.-H. Fan, Y.-N. Zhang, J.-P. Yu, M.-Y. Liu, W.-D. He, H.-C. Li, and W. Xiong, Nonreciprocal unconventional photon blockade with Kerr magnons, *Adv. Quantum Tech.* **7**, 2400043 (2024).
- [62] H.-Q. Zhang, S.-S. Chu, J.-S. Zhang, W.-X. Zhong, and G.-L. Cheng, Nonreciprocal magnon blockade based on nonlinear effects, *Opt. Lett.* **49**, 2009 (2024).
- [63] W. Zhang, S. Liu, S. Zhang, and H.-F. Wang, Magnon blockade induced by parametric amplification, *Phys. Rev. A* **109**, 043712 (2024).
- [64] W. Zhang, S. Liu, S. Zhang, and H.-F. Wang, Nonreciprocal unconventional magnon blockade induced by barnett effect and parametric amplification, *Opt. Express* **33**, 3339 (2025).
- [65] X. Deng, K.-K. Zhang, T. Shui, and W.-X. Yang, Nonreciprocal unconventional magnon blockade via the sagnac-fizeau shift in an optomagnonic system, *Phys. Rev. A* **110**, 063711 (2024).
- [66] Y. Li, T. Polakovic, Y.-L. Wang, J. Xu, S. Lendinez, Z. Zhang, J. Ding, T. Khaire, H. Saglam, R. Divan, J. Pearson, W.-K. Kwok, Z. Xiao, V. Novosad, A. Hoffmann, and W. Zhang, Strong coupling between magnons and microwave photons in on-chip ferromagnet-superconductor thin-film devices, *Phys. Rev. Lett.* **123**, 107701 (2019).
- [67] C. Zhang, C. Jia, Y. Shi, C. Jiang, D. Xue, C. K. Ong, and G. Chai, Nonreciprocal multimode and indirect couplings in cavity magnonics, *Phys. Rev. B* **103**, 184427 (2021).
- [68] D.-W. Luo, X.-F. Qian, and T. Yu, Optically mediated remote entanglement generation in magnon-cavity systems, *Phys. Rev. A* **109**, 012611 (2024).
- [69] J. Rao, C. Y. Wang, B. Yao, Z. J. Chen, K. X. Zhao, and W. Lu, Meterscale strong coupling between magnons and photons, *Phys. Rev. Lett.* **131**, 106702 (2023).
- [70] J. Yao, C. Lu, X. Fan, D. Xue, G. E. Bridges, and C.-M. Hu, Nonreciprocal control of the speed of light using cavity magnonics, *Phys. Rev. Lett.* **134**, 196904 (2025).
- [71] G. Zhao, Y. Wang, and X.-F. Qian, Theory of the magnon purcell effect in a cavity magnonic system, *Phys. Rev. B* **111**, 214428 (2025).
- [72] L. Bai, M. Harder, Y. P. Chen, X. Fan, J. Q. Xiao, and C.-M. Hu, Spin pumping in electro-dynamically coupled magnon-photon systems, *Phys. Rev. Lett.* **114**, 227201 (2015).
- [73] O. O. Soykal and M. E. Flatté, Strong field interactions between a nanomagnet and a photonic cavity, *Phys. Rev. Lett.* **104**, 077202 (2010).
- [74] D. Zhang, X.-Q. Luo, Y.-P. Wang, T.-F. Li, and J. You, Observation of the exceptional point in cavity magnon-polaritons, *Nat. Commun.* **8**, 1368 (2017).
- [75] B. Yao, Y. Gui, J. Rao, S. Kaur, X. Chen, W. Lu, Y. Xiao, H. Guo, K.-P. Marzlin, and C.-M. Hu, Cooperative polariton dynamics in feedback-coupled cavities, *Nat. Commun.* **8**, 1437 (2017).
- [76] N. Kostylev, M. Goryachev, and M. E. Tobar, Superstrong coupling of a microwave cavity to yttrium iron garnet magnons, *Appl. Phys. Lett.* **108**, 062402 (2016).
- [77] J. Bourhill, N. Kostylev, M. Goryachev, D. L. Creedon, and M. E. Tobar, Ultrahigh cooperativity interactions between magnons and resonant photons in a yig sphere, *Phys. Rev. B* **93**, 144420 (2016).
- [78] Y. Tabuchi, S. Ishino, T. Ishikawa, R. Yamazaki, K. Usami, and Y. Nakamura, Hybridizing ferromagnetic magnons and microwave photons in the quantum limit, *Phys. Rev. Lett.* **113**, 083603 (2014).
- [79] D. Zhang, X.-M. Wang, T.-F. Li, X.-Q. Luo, W. Wu, F. Nori, and J. You, Cavity quantum electrodynamics with ferromagnetic magnons in a small yttrium-iron-garnet sphere, *NPJ Quantum Inf.* **1**, 1 (2015).
- [80] X. Zhang, C.-L. Zou, L. Jiang, and H. X. Tang, Strongly coupled magnons and cavity microwave photons, *Phys. Rev. Lett.* **113**, 156401 (2014).
- [81] A. S. Kuznetsov, K. Biermann, A. A. Reynoso, A. Fainstein, and P. V. Santos, Microcavity phonoritons—a coherent optical-to-microwave interface, *Nat. Commun.* **14**, 5470 (2023).
- [82] R.-C. Shen, J. Li, Y.-M. Sun, W.-J. Wu, X. Zuo, Y.-P. Wang, S.-Y. Zhu, and J. You, Cavity-magnon polaritons strongly coupled to phonons, *Nat. Commun.* **16**, 5652 (2025).
- [83] J. Rao, S. Kaur, B. Yao, E. Edwards, Y. Zhao, X. Fan, D. Xue, T. J. Silva, Y. Gui, and C.-M. Hu, Analogue of dynamic hall effect in cavity magnon polariton system and coherently controlled logic device, *Nat. Commun.* **10**, 2934 (2019).
- [84] Z.-Q. Wang, Z.-Y. Wang, Y.-P. Wang, and J. Q. You, Single-mode magnon-polariton lasing and amplification controlled by dissipative coupling, *Phys. Rev. Lett.* **135**, 186704 (2025).
- [85] M.-L. Peng, M. Tian, X.-C. Chen, M.-F. Wang, G.-Q. Zhang, H.-C. Li, and W. Xiong, Cavity magnon-polariton interface for strong spin-spin coupling, *Opt. Lett.* **50**, 1516 (2025).
- [86] A. Delteil, T. Fink, A. Schade, S. Höfling, C. Schneider, and A. İmamoğlu, Towards polariton blockade of confined exciton-polaritons, *Nat. Mater.* **18**, 219 (2019).
- [87] Y.-P. Wang, G.-Q. Zhang, D. Zhang, T.-F. Li, C.-M. Hu, and J. Q. You, Bistability of cavity magnon polaritons, *Phys. Rev. Lett.* **120**, 057202 (2018).
- [88] J. B. Curtis, A. Grankin, N. R. Poniatowski, V. M. Galitski, P. Narang, and E. Demler, Cavity magnon-polaritons in cuprate parent compounds, *Phys. Rev. Res.* **4**, 013101 (2022).
- [89] J. Bourhill, W. Yu, V. Vlaminck, G. E. W. Bauer, G. Ruoso, and V. Castel, Generation of circulating cavity magnon polaritons, *Phys. Rev. Appl.* **19**, 014030 (2023).
- [90] Y. Zhang and Y. Xiao, Non-hermitian skin effect of the

- cavity magnon polariton, *Phys. Rev. Appl.* **23**, 044065 (2025).
- [91] T.-T. Ma, J. Tang, Y.-L. Zuo, R. Huang, A. Miranowicz, F. Nori, and H. Jing, Two-polariton blockade via ultrastrong light-matter coupling, *Phys. Rev. Lett.* **136**, 033601 (2026).
- [92] A. Karnieli, S. Tsesses, R. Yu, N. Rivera, A. Arie, I. Kaminer, and S. Fan, Universal and ultrafast quantum computation based on free-electron-polariton blockade, *PRX Quantum* **5**, 010339 (2024).
- [93] See supplemental material at [for the validation of the effective Hamiltonian and the derivation of the single-photon and single-magnon blockades.](#)
- [94] B. Zare Rameshti, S. Viola Kusminskiy, J. A. Haigh, K. Usami, D. Lachance-Quirion, Y. Nakamura, C.-M. Hu, H. X. Tang, G. E. Bauer, and Y. M. Blanter, Cavity magnonics, *Phys. Rep.* **979**, 1 (2022).
- [95] Y.-P. Wang, G.-Q. Zhang, D. Zhang, X.-Q. Luo, W. Xiong, S.-P. Wang, T.-F. Li, C.-M. Hu, and J. Q. You, Magnon kerr effect in a strongly coupled cavity-magnon system, *Phys. Rev. B* **94**, 224410 (2016).
- [96] C. Kong, H. Xiong, and Y. Wu, Magnon-induced nonreciprocity based on the magnon kerr effect, *Phys. Rev. Appl.* **12**, 034001 (2019).
- [97] Z.-B. Yang, H. Jin, J.-W. Jin, J.-Y. Liu, H.-Y. Liu, and R.-C. Yang, Bistability of squeezing and entanglement in cavity magnonics, *Phys. Rev. Res.* **3**, 023126 (2021).
- [98] C. Kong, X.-M. Bao, J.-B. Liu, and H. Xiong, Magnon-mediated nonreciprocal microwave transmission based on quantum interference, *Opt. Express* **29**, 25477 (2021).
- [99] J. Bourhill, V. Castel, A. Manchec, and G. Cochet, Universal characterization of cavity–magnon polariton coupling strength verified in modifiable microwave cavity, *J. Appl. Phys.* **128**, 073904 (2020).
- [100] Q. Bin, H. Jing, Y. Wu, F. Nori, and X.-Y. Lü, Nonreciprocal bundle emissions of quantum entangled pairs, *Phys. Rev. Lett.* **133**, 043601 (2024).
- [101] P. Forn-Díaz, L. Lamata, E. Rico, J. Kono, and E. Solano, Ultrastrong coupling regimes of light-matter interaction, *Rev. Mod. Phys.* **91**, 025005 (2019).
- [102] M. Goryachev, W. G. Farr, D. L. Creedon, Y. Fan, M. Kostylev, and M. E. Tobar, High-cooperativity cavity qed with magnons at microwave frequencies, *Phys. Rev. Appl.* **2**, 054002 (2014).
- [103] C. Zhang, Z. Hao, Y. Shi, X. Li, C. Jiang, C. Ong, D. Gao, and G. Chai, Simultaneous realization of nonreciprocal and ultra-strong coupling in cavity magnonics, *npj Spintronics* **3**, 45 (2025).
- [104] A. Grimm, N. E. Frattini, S. Puri, S. O. Mundhada, S. Touzard, M. Mirrahimi, S. M. Girvin, S. Shankar, and M. H. Devoret, Stabilization and operation of a Kerr-cat qubit, *Nature* **584**, 205 (2020).
- [105] X. He, Y. Lu, D. Bao, H. Xue, W. Jiang, Z. Wang, A. Roudsari, P. Delsing, J. Tsai, and Z. Lin, Fast generation of schrödinger cat states using a Kerr-tunable superconducting resonator, *Nat. Commun.* **14**, 6358 (2023).
- [106] A. Z. Ding, B. L. Brock, A. Eickbusch, A. Kootandavida, N. E. Frattini, R. G. Cortiñas, V. R. Joshi, S. J. de Graaf, B. J. Chapman, S. Ganjam, *et al.*, Quantum control of an oscillator with a Kerr-cat qubit, *Nat. Commun.* **16**, 5279 (2025).
- [107] D. Iyama, T. Kamiya, S. Fujii, H. Mukai, Y. Zhou, T. Nagase, A. Tomonaga, R. Wang, J.-J. Xue, S. Watabe, *et al.*, Observation and manipulation of quantum interference in a superconducting Kerr parametric oscillator, *Nat. Commun.* **15**, 86 (2024).
- [108] R. Hou, W. Zhang, X. Han, H.-F. Wang, and S. Zhang, Magnon blockade based on the Kerr nonlinearity in cavity electromagnonics, *Phys. Rev. A* **109**, 033721 (2024).
- [109] S.-W. Xu, Z.-Y. Zhang, J.-T. Ye, Z.-Z. Zhang, Y.-Y. Guo, K.-X. Yan, Y.-H. Chen, and Y. Xia, Optimal robust control of cat-state qubits against parameter imperfections, *Opt. Express* **33**, 40755 (2025).